Sensitivity analysis of circumferential transducer array with T(0,1) mode of pipes

Xudong Niu[1,2], Hugo R. Marques[2] and Hua-Peng Chen[*1]

[1]*Department of Engineering Science, University of Greenwich, Chatham, Kent ME4 4TB, UK*
[2]*TWI Ltd. Granta Park, Cambridge, Cambridgeshire CB21 6AL, UK*

Abstract. Guided wave testing is a reliable and safe method for pipeline inspection. In general, guided wave testing employs a circumferential array of piezoelectric transducers to clamp on the pipe circumference. The sensitivity of the operation depends on many factors, including transducer distribution across the circumferential array. This paper presents the sensitivity analysis of transducer array for the circumferential characteristics of guided waves in a pipe using finite element modelling and experimental studies. Various cases are investigated for the outputs of guided waves in the numerical simulations, including the number of transducers per array, transducer excitation variability and variations in transducer spacing. The effect of the dimensions of simulated notches in the pipe is also investigated for different arrangements of the transducer array. The results from the finite element numerical simulations are then compared with the related experimental results. Results show that the numerical outputs agree well with the experimental data, and the guided wave mode T(0,1) presents high sensitivity to the notch size in the circumferential direction, but low sensitivity to the notch size in the axial direction.

Keywords: guided wave; piezoelectric transducer array; finite element modelling; wave propagation; pipeline; structural integrity

1. Introduction

Structural integrity evaluation of oil and gas pipelines with ultrasonic guided wave is particularly attractive, since serious incidents of structural failure may occur owing to loss of pipe wall thickness by corrosion, fatigue cracks or manufacture anomalies. Among non-destructive testing (NDT) methods, commonly used techniques include X-ray inspection, ultrasonic testing (UT), and guided wave (GW) testing. Compared with UT, GW testing makes use of lower frequency elastic waves, typically from 20 *kHz* to 100 *kHz* (Mudge 2001). Guided wave has an advantage to allow for long distance (many tens of metres) wave propagation along a pipeline, with minimal attenuation under ideal conditions. Furthermore, GW can propagate with a high susceptibility to interference (Liu and Kleiner 2013). In practices, GW systems typically take the form of a circumferential array tool (Cawley *et al.* 1994) that is dry-coupled to the pipeline.

Piezoelectric transducers have been investigated in many studies such as Sung and Tien (2015) and Zhou *et al.* (2016), and used widely to excite guided waves for structural health monitoring and NDT of different structures, such as beams (Karayannis *et al.* 2015), plates (Muralidharan *et al.* 2008) and pipelines (Lee and Sohn 2012, Hong *et al.* 2016). In GW testing, the dry-coupled piezoelectric transducer system (Alleyne and Cawley, 1996) has some advantages, including simple, light and readily removable in the pipe inspection. For the defects on the

external and internal surfaces of pipe structures, the behaviour of the different GW modes with a variety of defects was characterised by Alleyne and Cawley (1992). Circumferential transducer arrays allow for the generation of an axisymmetric wave mode and the suppression of non-axisymmetric wave modes (Cawley 2007, Løvstad and Cawley 2011). This effective system is able to minimise undesired wave modes using GW testing for pipeline inspections. By using long range GW testing, Alleyne and Cawley (1997) identified effectively corrosion defects using cylindrical wave mode. Results were presented where GW is employed to identify circumferential cracks including axial cracks (Luo *et al.* 2005), circumferential notches (Demma *et al.* 2004) and longitudinal notches (Liu *et al.* 2006). Sharan *et al.* (2015) described that a 3–9% defect of cross-sectional area of a pipe can be detected using GW testing, depending on the signal-to-noise ratio. The enhancement of the level of sensitivity in pipeline inspection is an area of interest for the industry. This can be achieved by optimising the circumferential transducer array design to increase performance without significant increase in manufacturing and testing costs.

The wave propagation in pipes and GW testing for structural integrity evaluation have been widely investigated. Gazis (1959) investigated the propagation of three families of guided wave modes in pipe-like structures. Meitzler (1961) studied the propagation behaviour of guided wave modes in a cylindrical solid through further experimental studies. Mohr and Holler (1976) investigated cylindrical wave modes propagating in small-diameter metal tubes by GW testing. Later, Silk and Bainton (1979) developed the GW testing of metal tube structures and tested the structures using piezoelectric transducer probes.

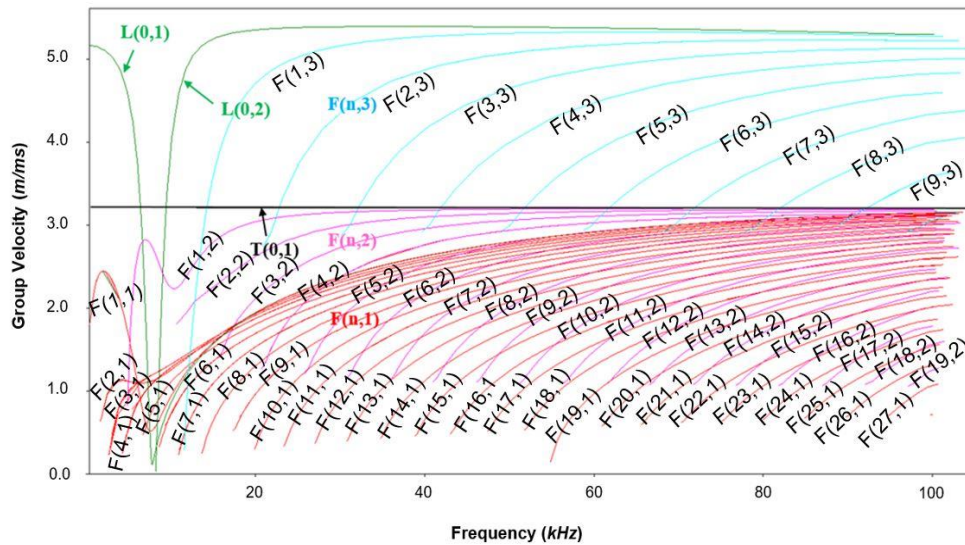*Corresponding author, Research Professor
 E-mail: hp.chen@outlook.com

Fig. 1 Group velocity dispersion curves for an 8-inch schedule 40 steel pipe

Field tests using the initial commercialised devices were described by Alleyne *et al.* (2001) and Mudge (2001), respectively. Recently, the transducer array has been designed to investigate the ultrasound (Luo and Rose 2007, Davies and Cawley 2009, Catton and Kleiner 2005) at points around the circumference of the pipe by the advanced 'focusing' technology. In order to describe GW modes in pipes a nomenclature of $Y(n, m)$ is introduced (Silk and Bainton 1979), in which Y represents the guide wave mode operation, namely L, T or F for longitudinal, torsional or flexural wave modes, respectively, and n indicates the circumferential order and m indicates the mode order of occurrence. Fig. 1 shows the results for group velocity dispersion curves for an 8-inch (219.1 *mm* outer diameter) and schedule 40 (8.18 *mm* wall thickness) steel pipe. These dispersion curves were generated by DISPERSE (Pavlakovic *et al.* 1997) software. In this range of frequencies, it can be seen that the longitudinal wave modes L(0,1) and L(0,2) are followed by flexural wave modes F(n,1) and F(n,3), respectively. The torsional wave mode T(0,1) also exists a 'family' flexural wave modes F(n,2).

For a selection of guided wave modes in pipe inspections, Yu *et al.* (2013) found that L(0,2) mode is the favourable one with the fastest group velocity in the multi-layered pipe with weak interface, when longitudinal guided waves are used in defect detection. Leinov *et al.* (2015) presented that L(0,2) wave mode also has lower attenuation values than the mode T(0,1) for GW testing in pipe buried in sand. In addition, the wave mode L(0,1) is promising in the ultrasonic guided wave testing through a combination of appropriate frequency selection and signal processing procedures. Izadpanah *et al.* (2008) found that the wave mode L(0,1) has a small variation of speed with frequency, and the compression transducers can excite the wave mode L(0,1) in isolation.

Recently, the fundamental torsional wave mode T(0,1) is often utilized for guided wave testing (Mudge 2001). The torsional wave mode T(0,1) has a constant phase/group velocity and is completely non-dispersive at all frequencies. Also, the torsional mode T(0,1) can propagate along pipes filled with liquid without any interference, when compared with L(0,2). Furthermore, the wave mode T(0,1) is much simple in transduction since no higher torsional wave modes exist at low frequencies. Research showed that the mode T(0,1) is an axisymmetric wave mode and the mode F(1,2) is a non-axisymmetric wave mode, as shown in Fig. 2. In general, a single axisymmetric wave mode T(0,1) can be generated if the transducer array has equal spacing across all transducers. In the cases without equal spacing, the non-axisymmetric wave modes F(n,2) may be more predominant.

To excite a single torsional wave T(0,1) mode, Rose (2014) simulated 8 transducers for a circumferential array around a 4-inch schedule 40 steel pipe. Volker and Vos (2012) used a ring of 32 transducers for an experiment of a steel pipe with defects. Also, Miao *et al.* (2017) presented the tangential displacement angular profile simulations of wave mode T(0,1) by different number of transducers (e.g., 1, 4, 8, 12, 24 and 32). These results show that the number of transducers has influence on quality of an excitation signal. In addition, research showed that a ring of 24 transducers can excite and receive a single T(0,1) in an aluminum pipe. A completed circle for the displacement profile was generated when no defect exists in the structure. A single torsional wave mode T(0,1) was evaluated from 24 transducers equally spaced on a 6-inch schedule 120 steel pipe circumference (Niu *et al.* 2017a). Therefore, a ring of 24 transducers is feasible in the aspect of technical application or commercial consideration for pipe inspection. The performance optimisation of piezoelectric transducer arrays in pipes can be achieved through a combination of finite element (FE) simulations and experimental testing.
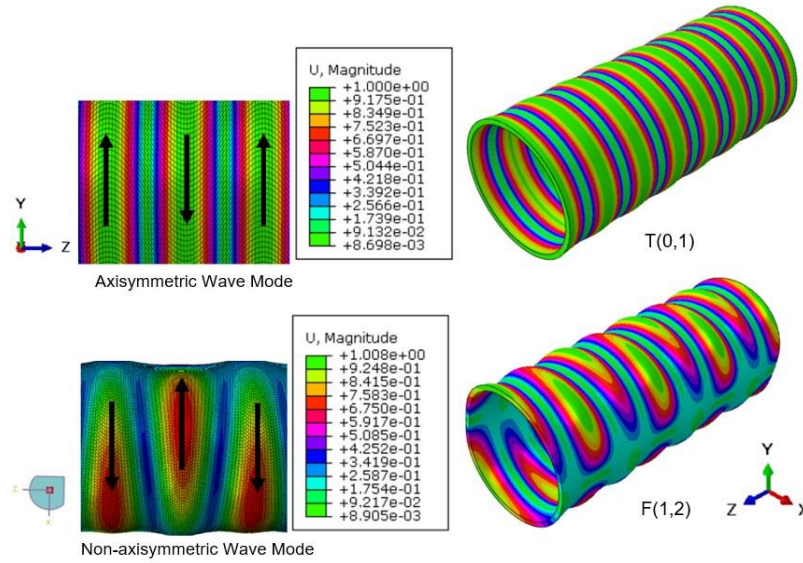
Fig. 2 Displacement characteristics of guided wave T(0,1) and F(1,2) modes in a steel pipe

The FE modelling has been widely used to simulate propagation of GW mode shapes (Niu *et al.* 2017a, Lowe *et al.* 2014, Fateri *et al.* 2015, Niu *et al.* 2017b) and their interaction with defects in pipes (Duan and Kirby 2015, Duan *et al.* 2017, Duan *et al.* 2016). Experimental testing was operated using 3D scanning laser Doppler vibrometer (LDV) (Jenal *et al.* 2010) or 3D compact laser vibrometer (CLV) (Niu *et al.* 2017b, Niu *et al.* 2017c).

This paper presents sensitivity analysis of GW testing towards the optimisation of transducer arrays for pipe inspection. Numerical simulations using FE method and experimental validation by 3D laser vibrometer systems are employed in this study. Guided waves propagation is undertaken on a 4450 *mm* long, 8-inch (219.1 *mm* outer diameter), schedule 40 (8.18 *mm* wall thickness) steel pipe. The simulated transducer array design is based on a commercially available tool incorporating three circumferential arrays, also known as rings. Each ring includes 24 piezoelectric transducers exciting the fundamental torsional wave mode T(0,1). Here, numerical simulations for a 33-degree spacing between the start and end transducers of the array for inspecting an 8-inch steel pipe are undertaken for practical uses. The uneven distribution of transducers on the array causes the excitation of not only the T(0,1) mode but also the excitation of non-axisymmetric 'family' of flexural wave modes F(*n*,2). Finally, the sensitivity of defect on a circumferential array design is studied, and the influence of spacing between the start and end transducers in a circumferential array is also investigated, where the T(0,1) and F(*n*,2) proportion of circumferential wave mode interaction with a simulated notch is considered.

2. Guided wave propagation

2.1 Equations of motion

The theoretical background has been developed for guided wave propagation in the axial direction of a pipe-like structure. The structure is assumed as an elastic isotropic hollow cylinder with traction-free boundary conditions. The governing equation for guided wave propagation in the elastic medium can be expressed as follows (Gazis 1959)

$$(\lambda + \mu)\nabla\nabla \cdot \overline{U} + \mu\nabla^2\overline{U} = \rho\frac{\partial^2\overline{U}}{\partial t^2} \tag{1}$$

where t indicates the time, $\overline{U}$ represents the displacement vector, ρ represents the density and λ and μ are Lamé constants. ∇^2 represents the three-dimensional Laplace operator. Eq. (1) can be rewritten as follows using a Cartesian coordinate system

$$(\lambda+\mu)\frac{\partial}{\partial X}\left(\frac{\partial U_X}{\partial X}+\frac{\partial U_Y}{\partial Y}+\frac{\partial U_z}{\partial Z}\right)+\mu\left(\frac{\partial^2}{\partial X^2}+\frac{\partial^2}{\partial Y^2}+\frac{\partial^2}{\partial Z^2}\right)U_X=\rho\frac{\partial^2 U_X}{\partial t^2} \tag{2a}$$

$$(\lambda+\mu)\frac{\partial}{\partial Y}\left(\frac{\partial U_X}{\partial X}+\frac{\partial U_Y}{\partial Y}+\frac{\partial U_z}{\partial Z}\right)+\mu\left(\frac{\partial^2}{\partial X^2}+\frac{\partial^2}{\partial Y^2}+\frac{\partial^2}{\partial Z^2}\right)U_Y=\rho\frac{\partial^2 U_Y}{\partial t^2} \tag{2b}$$

$$(\lambda+\mu)\frac{\partial}{\partial X}\left(\frac{\partial U_X}{\partial X}+\frac{\partial U_Y}{\partial Y}+\frac{\partial U_z}{\partial Z}\right)+\mu\left(\frac{\partial^2}{\partial X^2}+\frac{\partial^2}{\partial Y^2}+\frac{\partial^2}{\partial Z^2}\right)U_Z=\rho\frac{\partial^2 U_Z}{\partial t^2} \tag{2c}$$

where U_X, U_Y and U_z are guided wave mode particle displacement components. Since the cylindrical structure considered is isotropic, the expression of the displacement field can be simplified by Helmholtz decomposition

$$\overline{U} = \nabla\Phi + \nabla \times \overline{V} \tag{3}$$

where Φ represents a dilatational scalar potential and $\overline{V}$ represents an equivoluminal vector potential. It is assumed that the pipe-like structure is infinitely long with traction-free boundary conditions on the inner and outer surfaces.
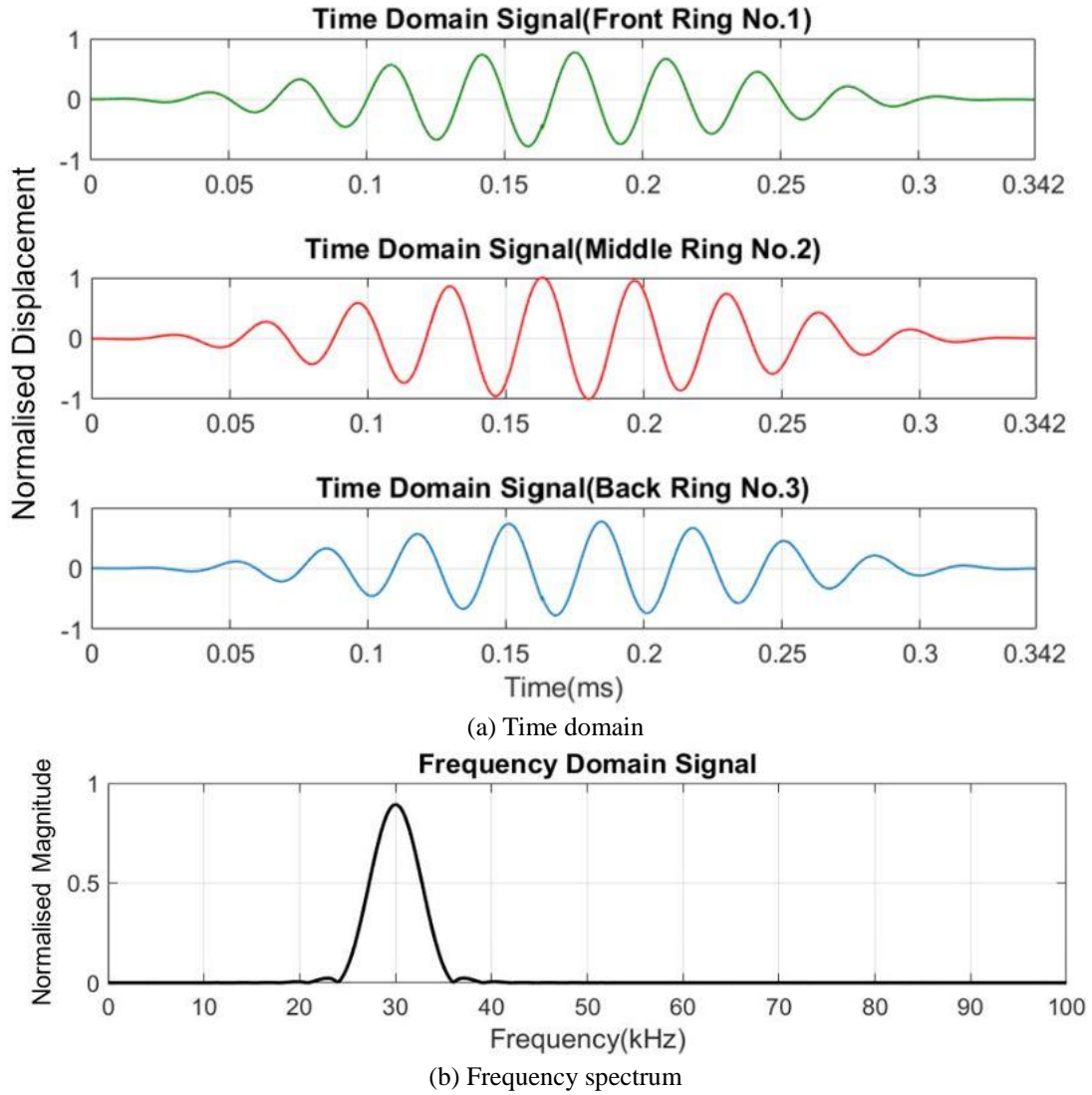
(a) Time domain

(b) Frequency spectrum

Fig. 3 Guided wave signal excitations for three rings

By using gauge invariance condition, the problem can be solved without considering the boundary conditions. On the basis of elasticity, the related potentials of $\overline{V}$ and Φ can be expressed as

$$\frac{\partial^2 \Phi}{\partial R^2} + \frac{1}{R}\frac{\partial \Phi}{\partial R} + \frac{1}{R^2}\frac{\partial^2 \Phi}{\partial \theta^2} + \frac{\partial^2 \Phi}{\partial Z^2} = \frac{1}{c_L}\frac{\partial^2 \Phi}{\partial t^2} \qquad (4a)$$

$$\nabla^2 (V_R \overline{e}_R + V_\theta \overline{e}_\theta + V_Z \overline{e}_Z) = \frac{1}{c_T}\frac{\partial^2 \overline{V}}{\partial t^2} \qquad (4b)$$

where $c_L = \sqrt{\lambda+2\mu/\rho}$ is the dilatational longitudinal bulk wave velocity and $c_T = \sqrt{\mu/\rho}$ is the shear bulk wave velocity; $\overline{e}_R$, $\overline{e}_\theta$, and $\overline{e}_Z$ represent the cylindrical coordinates in the radial, circumferential and axial directions, respectively. To separate variables, it is assumed by Gazis (1959) that

$$\Phi = f(R)cos(n\theta)e^{i(kZ-\omega t)} \qquad (5a)$$

$$V_R = v_R(R)sin(n\theta)e^{i(kZ-\omega t)} \qquad (5b)$$

$$V_\theta = v_\theta(R)cos(n\theta)e^{i(kZ-\omega t)} \qquad (5c)$$

$$V_Z = v_Z(R)sin(n\theta)e^{i(kZ-\omega t)} \qquad (5d)$$

From Eq. (5), the displacement components can be expressed as (Rose 2014)

$$U_R = A_R(R)cos(n\theta)e^{i(kZ-\omega t)} \qquad (6a)$$

$$U_\theta = A_\theta(R)sin(n\theta)e^{i(kZ-\omega t)} \qquad (6b)$$

$$U_Z = A_Z(R)cos(n\theta)e^{i(kZ-\omega t)} \qquad (6c)$$

where the terms of U_R, U_θ and U_Z are the components of displacement in the radial, circumferential and axial directions, respectively. The terms of $A_R(R)$, $A_\theta(R)$ and

$A_Z(R)$ are the corresponding displacement amplitudes composed of Bessel functions in the out-of-plane. The non-negative integer n (=0, 1, 2, 3, …) represents the mode circumferential order, and kZ represents the angular wavenumber in the axial (Z) direction.

The procedure describe above is used to solve the governing equations for the displacement components. In finite element modelling, the governing equations can be decomposed differently. The details of the numerical modelling can be found in Hua *et al.* (2010) and Duan *et al.* (2016). Furthermore, the above equations are based on the exact three-dimensional theory of elasticity. It is possible to simplify the equations by making use of certain approximations in the thickness direction of the pipe, and details of the simplified theories can be found in Muggleton *et al.* (2002).

2.2 Excitation for wave modes

In the numerical simulations, the modelled transducer array was excited with a 10 cycle pulse at 30 *kHz* to generate the torsional wave mode T(0,1). This wave mode causes in-plane angular displacements in the cylindrical coordinate system. The frequency of 30 *kHz* was chosen as a low-frequency signal in the range of operating frequencies. The selected number of cycles was aimed at reducing the signal bandwidth to prevent excitation of other undesired modes. The excitation was undertaken by a Hanning windowed tone burst signal, given by

$$F(t) = \frac{1}{2}\left[1 - cos\left(\frac{2\pi f t}{n}\right)\right]sin(2\pi f t) \qquad (7)$$

where t is the time, f is the centre frequency of the wave mode, and n is the number of the signal cycles.

The excitation of three transducer rings by a 30 *kHz*, 10-cycle Hanning windowed pulse in the time and frequency spectrum is shown in Figs. 3(a) and 3(b). These three circumferential rings are named as Ring No.1, Ring No.2 and Ring No.3, respectively. These rings with distances of 30 *mm* are installed at the front, middle and back of the tool along the pipe, respectively. The wave mode T(0,1) and its interaction with modes F(*n*,2) are transmitted by circumferential motion at this frequency. The three rings were excited with various signals. Ring No.1 was excited by signal given in Eq. (7). The signal of Ring No.2 was inverted when compared with the signal of Ring No.1. The signal of Ring No.3 was time-delayed and the time is the ring distance of 30 *mm* divided by phase velocity of wave mode T(0,1). The use of three rings aims to cancel the undesired modes and control the wave propagation direction of the selected mode.

2.3 Transducer array

To describe distribution locations of a group of transducers in an array around a pipe in the circumferential direction, a relationship can be given as

$$C_z(\alpha) = \begin{cases} \dfrac{2\pi}{N} & (\alpha = \alpha', N \geq 1) \\ \dfrac{2\pi - \alpha'}{N-1} & (\alpha \neq \alpha', N \geq 2) \end{cases} \qquad (N = 1,2,3,...,n) \qquad (8)$$

where $C_z(\alpha)$ is superposition of the circumferential distribution of all transducers at the distance z along the pipe, α is the radian of transducers spacing, α' is the radian of gap between the start and end of transducer array in a ring, and N is the number of transducer in a ring array.

3. Finite element numerical modelling

3.1 Transducer array modelling

Figs. 4(a) and 4(b) show an overview of FE simulations setup with GW propagation along a 4450 *mm* long, 8-inch, schedule 40 steel pipe in pitch-catch testing operation. The steel pipe was modelled as a linear isotropic material with a mass density $\rho = 7850$ kg/m^3, Young's modulus $E = 210$ *GPa* and Poisson's ratio $v = 0.3$. At the left end of the pipe, three circumferential arrays, composed of 24 transducers equally spaced except for 33-degree spacing between the start and end transducers, were excited by a 10-cycle Hanning windowed pulse with centre frequency of 30 *kHz* and bandwidth of ± 6 *kHz*. A circumferential transducer array is considered as excitation, and the transducers are modelled as point sources. The receiving array, composed of 24 uniformly spaced point receivers, is located at 2000 *mm* away from the left end of pipe model. A mesh with a total of 324,064 Hex elements is generated, to ensure a minimum of 8 elements per wavelength for satisfactory accuracy (Fateri *et al.* 2015, Alleyne *et al.* 1998). An average mesh size of 4.5 *mm* and a step time of 186 *ns* are used in the simulations. The ultrasonic signal is introduced as a concentrated force distributed uniformly at point sources in the circumferential direction. The transmitted signal is excited, and the guided wave propagates along the pipe from the left end of the pipe. The results show the torsional wave mode T(0,1) propagates by the circumferential arrays with a significantly higher amplitude, comparing with other modes.

Fig. 5(a) shows a time-displacement plot for No.1 receiver measured at 2000 *mm* away from the left end of the pipe and located at 82.5 degrees in the pipe profile. The impulse time of transmitted signal is 333 *μs*, the time-period of wave propagation is 3.4 *ms*. The FE results for the amplitude of displacements are transformed in the local cylindrical coordinate system *R* (radial), *T* (circumferential) and *Z* (axial) using MATLAB software. The spacing of 33 degrees between transducers cause the poor suppression of undesired wave modes F(*n*,2). The excited torsional wave mode T(0,1) transmits with a family of flexural wave modes F(*n*,2) on the pipe model. After that, the displacement values increase at the reflection from the pipe end because of the superposition of wave modes. Fig. 5(b) shows a polar plot of the maximum values for displacement in the circumferential direction at each of the 24 receiving
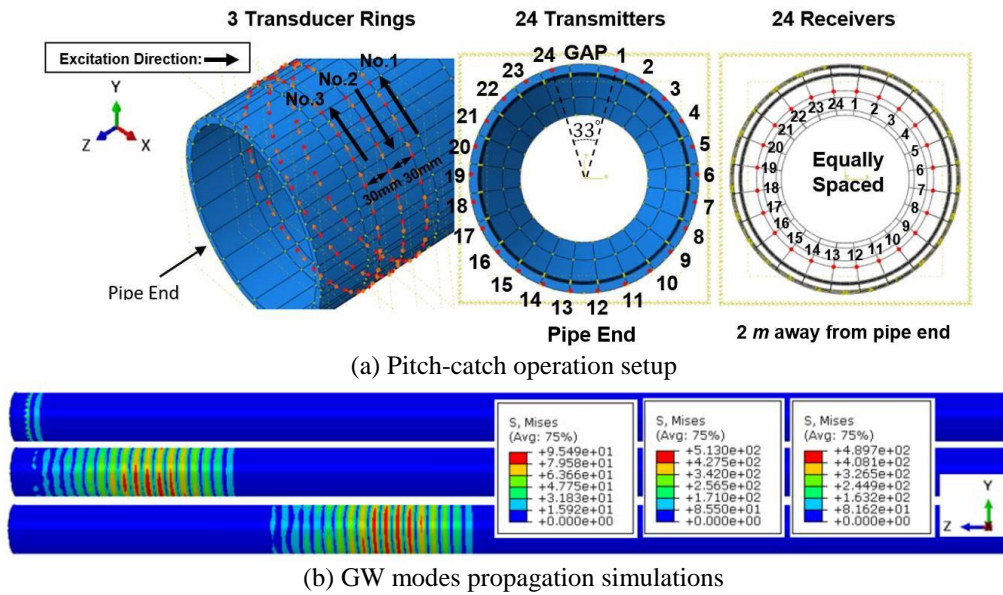
(a) Pitch-catch operation setup

(b) GW modes propagation simulations

Fig. 4 The FE modelling for an 8-inch, schedule 40 steel pipe

(a) Time-displacement record

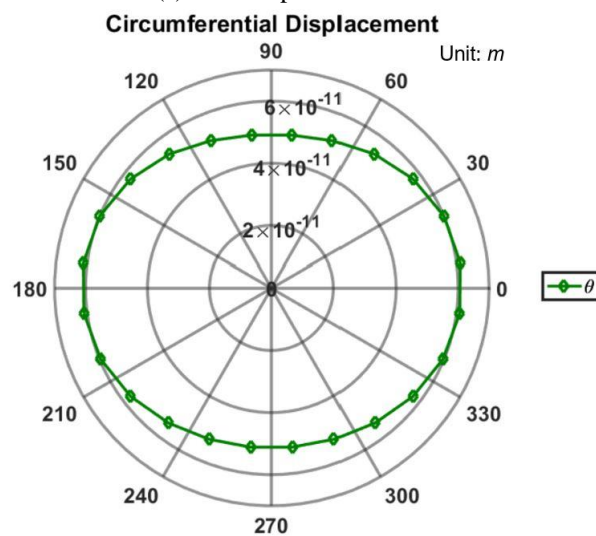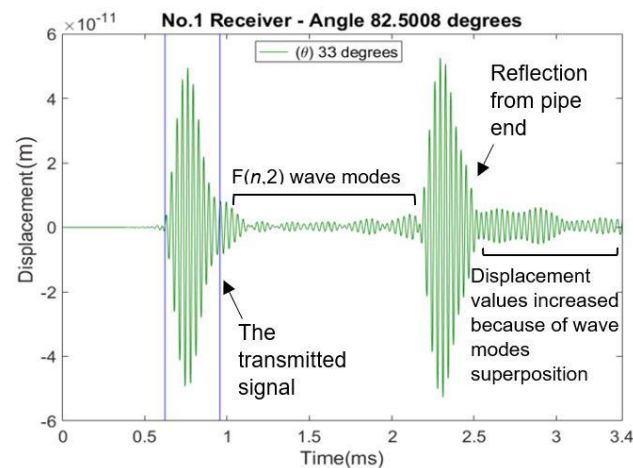(b) Polar plot of maximum circumferential displacements at each of the 24 receivers

Fig. 5 FE results for GWs transmitting along a pipe by circumferential arrays for pitch catch operation
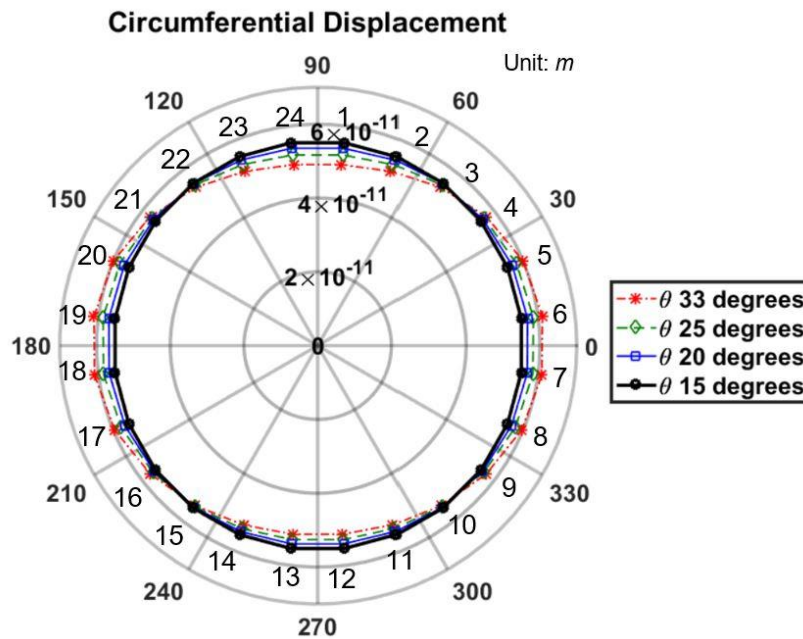
Fig. 6 Polar plot of all maximum circumferential displacements measured at all 24 receivers

transducers for the transmitted signal within the time window. The mode T(0,1) interacts with unwanted flexural wave modes F(n,2), leading to the variation of displacement amplitude in the circumferential direction, thus an imperfect circle shape is generated.

When the spacing between No.1 and No.24 transducers is 15 degrees around the pipe profile, the array of 24 transducers can be equally spaced and the distribution of transducers becomes an axisymmetric arrangement. The displacement amplitude is constant across all the receivers in the circumferential direction. Therefore, the influence of transduce spacing can be evaluated when the gap is reduced from 33 degrees to 25, 20 and finally 15 degrees, as shown in Fig. 6. It is noted that the displacement amplitude increases at transducers located approximately at 90 degrees and 270 degrees, while for the transducers located approximately at 0 degree and 180 degrees, the amplitude shows a remarkable reduction. From the results, a high purity for wave mode T(0,1) can be achieved when transducer is equally spaced on an array around a pipe.

3.2 Evaluation of flexural wave modes F(n,2) family

In order to ensure that a single wave mode T(0,1) is achieved, the wave modes of a pipe are separated by Fourier analysis using an array of 24 transducers equally spaced on the pipe. The family of flexural wave modes F(n,2) is investigated by reducing the gap spacing (from 33 degrees to 15 degrees) between No.1 and No.24 transducers of the array. Fig. 7(a) shows the results for the circumferential displacement amplitudes of the torsional wave mode T(0,1) with flexural wave modes F(n,2) at No.1 receiver in the case with a gap of 33 degrees. The data are recorded at 2.12 *ms* to obtain measurements before any

reflection from the other pipe end. Fourier analysis is used to produce the related results for 24 receivers, as given in Figs. 7(b) and 7(c). A group of circumferential orders up to 12 for the case is tested. The simulated transducer array is excited with a 10 cycle pulse at 30 *kHz* to generate the torsional wave mode T(0,1). The circumferential orders up to 7 for the range of frequencies from 24 *kHz* to 36 *kHz* can then be evaluated through investigations shown in Fig. 1. From the range of circumferential orders, the flexural wave modes F(1,2), F(2,2), F(7,2) are considered because of their effective proportion rate of normalised amplitude (higher than 1%), as shown in Fig. 7(b).

The flexural order modes are further studied for the case with a gap of 20 degrees spacing between No.1 and No.24 transducers, as shown in Fig. 8. The results show that only the flexural wave mode F(1,2) needs to be considered due to its proportion rate (approximately 1.6%).

From the results in Figs. 9(a) and 9(b), a single torsional wave mode T(0,1) can be achieved when transducers are equally spaced for an array around the pipe. Therefore, the design of transducer array is useful for axisymmetric structures, and it can suppress effectively other undesired wave modes using a transducer array equally spaced on a pipe.

3.3 Modelling of array sensitivity for circumferential notch detection

To investigate the sensitivity of a transducer array with an odd spacing between top two transducers for defect detection, a steel pipe with a circumferential notch was modelled. Fig.10(a) shows the FE model for a 4450 *mm*, 8-inch, schedule 40 steel pipe with a notch of 75 degrees (arc length of 143.5 *mm*)×10 *mm* in width along the axial

(a) Time-displacement plot

(b) Rectified waveforms and scaled waveforms of flexural mode F(*n*,2)

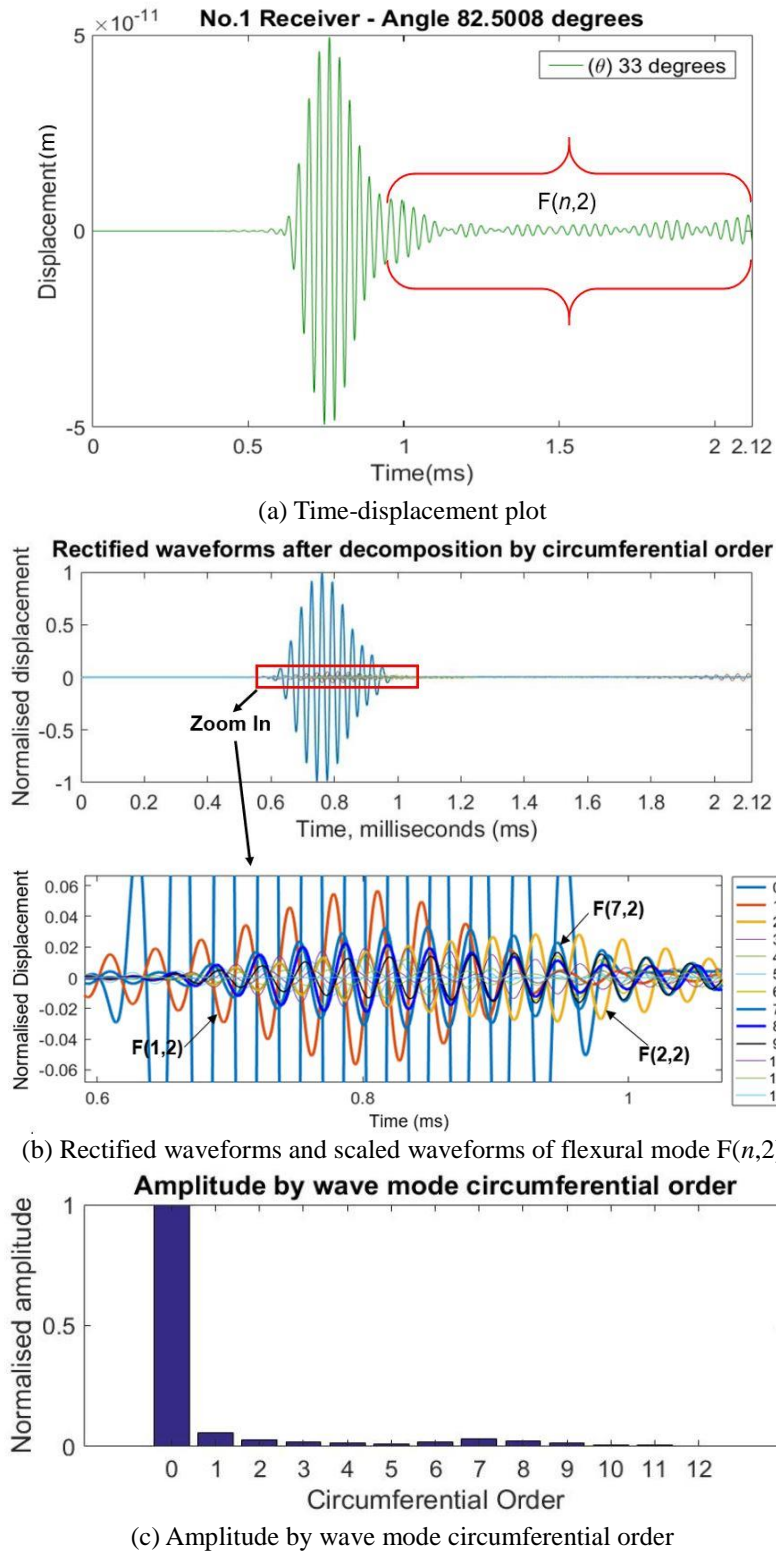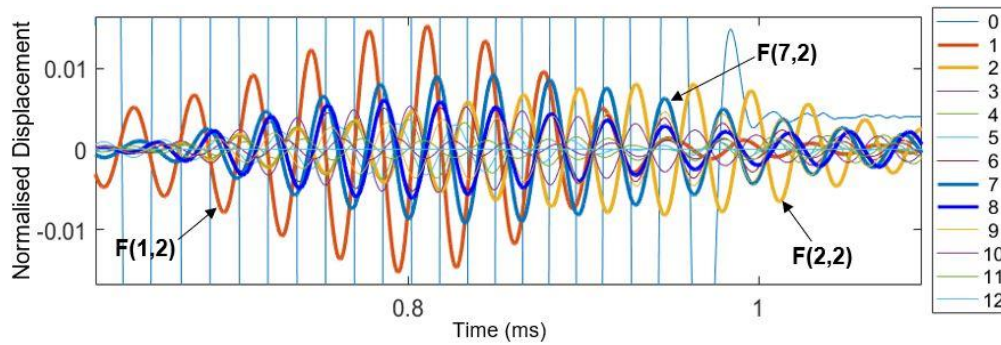(c) Amplitude by wave mode circumferential order

Fig. 7 Results for F(*n*,2) wave modes from 24 receivers generated by an array with an odd gap of 33 degrees spacing between No.1 and No.24 transducers

direction × 8.18 *mm* in thickness of the notch. The circumferential notch is assumed at the top of the steel pipe, and the notch is located at 1000 *mm* away from the array of 24 receivers. The transducers are modelled as point sources.

A pulse signal of 30 *kHz* is excited and propagates along the pipe. A total of 321,248 elements are generated for the FE modelling with an average mesh size of 4.5 *mm*. A step time of 186 *ns* is adopted. Figure 10(b) shows the T(0,1) with

Fig. 8 Results for F(*n*,2) wave modes from 24 receivers generated by an array with an odd gap of 20 degrees spacing between No.1 and No.24 transducers, scaled waveforms of flexural mode F(*n*,2)
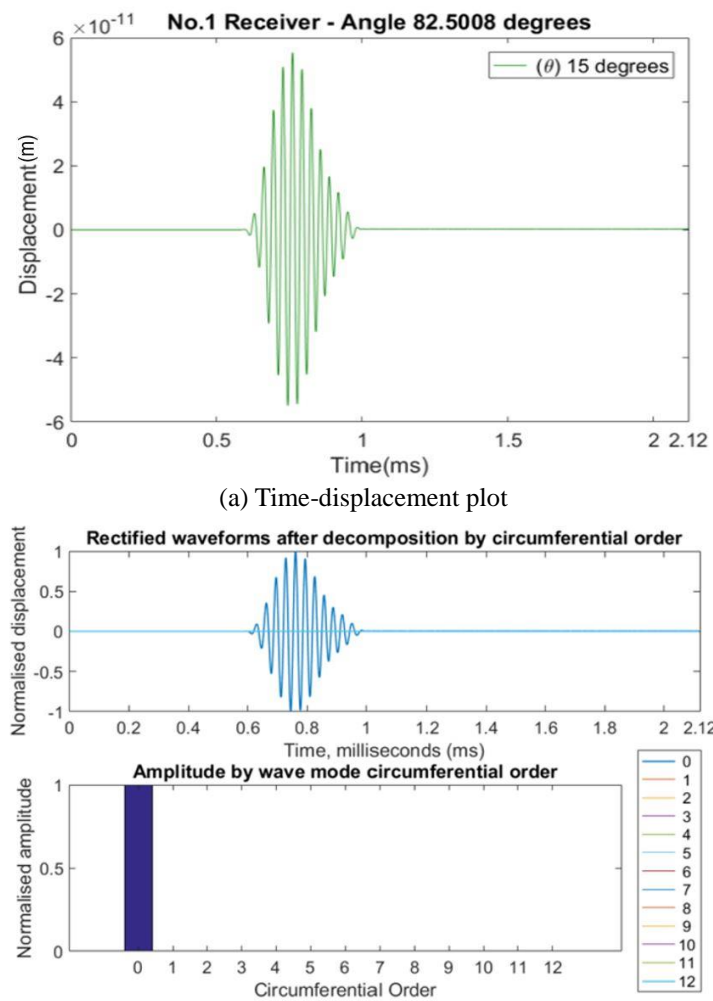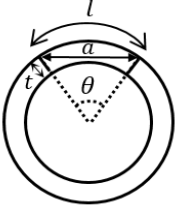

(a) Time-displacement plot

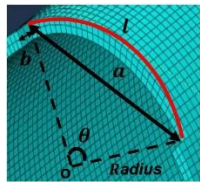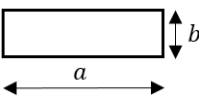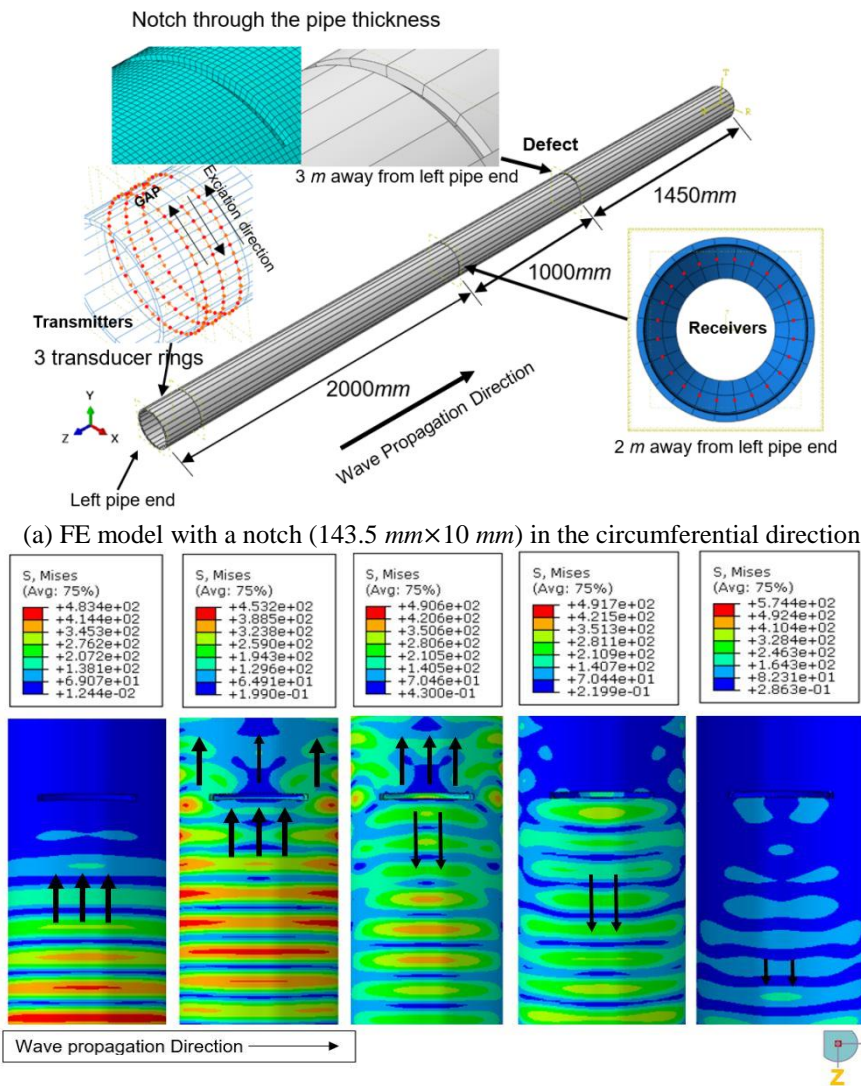(b) Rectified waveforms and amplitude by wave mode circumferential order

Fig. 9 Results for F(*n*,2) wave modes from 24 receivers generated by an array of equally spaced transducers

some flexural modes propagating on the pipe and the interaction with the circumferential notch. The wave modes are partially reflected from the circumferential notch. The sensitivity of the transducer array is analysed by reducing the spacing between No.1 and No.24 transducers from 33 degrees to 15 degrees.

A group of notch sizes with various dimensions are simulated to investigate the influence of notch size on wave propagation in the pipe. A total of four notch sizes are assumed for the cases with various transducer array arrangements and their details are described in Table 1.

Table 1 Simulated 3-dimensional notches with different sizes

Details of Notch Sizes						
Section profile	3D view	No.	θ_n (degree,°)	l_n (arc length, *mm*)	b_n (width, *mm*)	t_n (thickness, *mm*)
		1	15	28.7	10	8.18
		2	45	86.1	10	8.18
Vertical view		3	75	143.5	10	8.18
		4	75	143.5	20	8.18

(a) FE model with a notch (143.5 *mm*×10 *mm*) in the circumferential direction
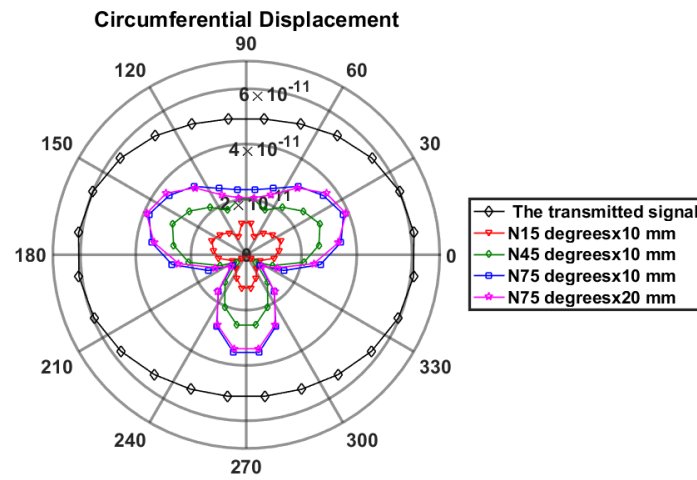

(b) Guided wave modes propagation and its interaction with the notch

Fig. 10 FE model of steel pipe with a circumferential notch
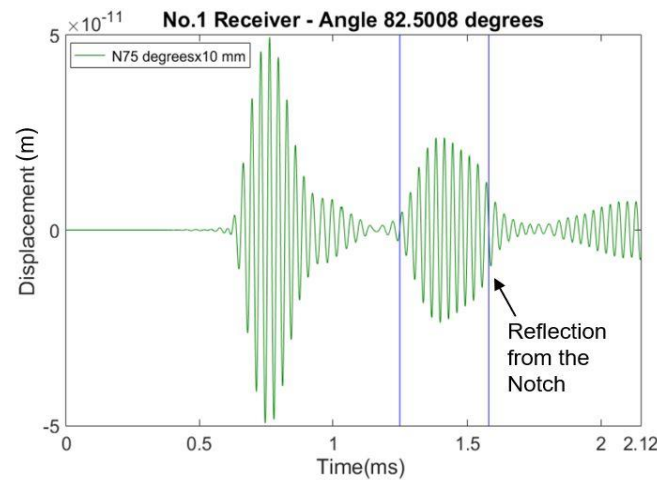
(a) Time-displacement data

(b) Polar plot for all measured maximum displacements in the circumferential direction
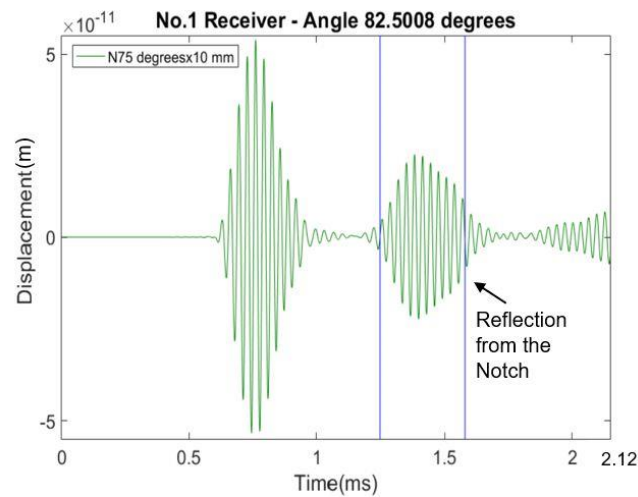
Fig. 11 Reflection from the notch using a circumferential array with a gap of 33 degrees spacing between No.1 and No.24 transducers

Three notch sizes in the circumferential direction (15 degrees, 45 degrees and 75 degrees in the pipe profile) are considered, and different notch widths in the axial direction (10 *mm* and 20 *mm* along the pipe) are discussed. These different notch dimensions are named here as N15 degrees×10 *mm*, N45 degrees×10 *mm*, N75 degrees×10 *mm* and N75 degrees×20 *mm*, respectively.

Figs. 11(a) and 11(b) show the results for the mode T(0,1) with F(n,2) amplitude of circumferential displacements for defect detection. The circumferential displacement amplitudes for the transmitted signal and reflection from the notch (N75 degrees×10 *mm*) at No.1 receiver, which are plotted in Fig. 11(a). The related data are recorded at 2.12 *ms* before any reflection from another pipe end. For the case of an array with 33 degrees spacing between No.1 and No.24 transducers, a polar plot for all the measured maximum displacements for the different notch sizes in the circumferential direction is presented in Fig. 11(b). The amplitude of the mode T(0,1) with modes F(n,2) increases as the notch grows in the circumferential direction at approximately 30 degrees, 90 degrees, 150 degrees and 270 degrees. The notch growth in the axial direction from 10 to 20 *mm* has small amplitude changes for the wave modes. Furthermore, the amplitude reduces slightly at approximately 90 degrees when the notch grows in the axial direction.

Figs. 12(a) and 12(b) give results for a single T(0,1) displacement amplitude in the circumferential direction. The circumferential displacement amplitudes at No.1 receiver in the case with notch N75 degrees×10 *mm* which are plotted in Fig. 12(a). From the results in Figs. 11-12, the circumferential displacement amplitudes of the transmitted signal increase and the value of the reflection from the notch reduces, when the spacing between two transducers located on either side of the 90 degrees decreases. Meanwhile, the amplitudes of dispersed wave modes reduce. Also, the amplitudes of the mode T(0,1) with modes F(n,2) increase as the spacing between No.1 and No.24 transducers reduces, since the amplitudes increase at approximately 90 degrees in the case with no defect.

(a) Time-displacement data
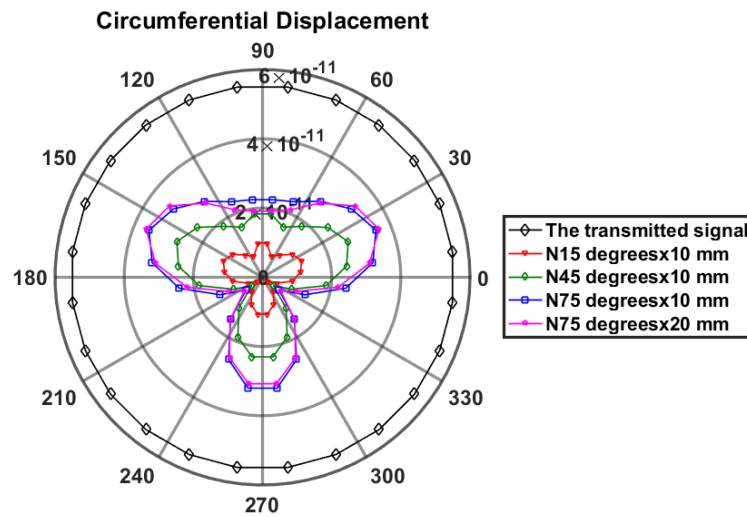
(b) Polar plot for all measured maximum displacements in the circumferential direction

Fig. 12 Reflection from the notch using an array of equally spaced transducers

Further studies show that the circumferential displacement amplitudes are very close to each other in the time-displacement records and in the related polar plots for different notch sizes, when the spacing between No.1 and No.24 transducers is within the range between 20 degrees and 15 degrees. Only the flexural wave mode F(1,2) needs to be considered due to its relatively higher proportion rate (approximately 1.6%). Thus, when the mode F(1,2) has its proportion rate less than 1.6%, the influence of the flexural wave mode on the notch could be negligible.

Figs. 13(a)-13(d) show results for a group of displacement amplitudes for reflection from the notch with different sizes in the circumferential direction. By considering different notch sizes, FE models are adopted for various transducer arrays with a gap reducing from 33 degrees to 15 degrees between No.1 and No.24 transducers. The results indicate that the sensitivity of transducer array can be minimised for all notch sizes, when the odd spacing has 20 degrees or is equally spaced around the pipe, despite the notch sizes. Also, no significant difference in amplitude

exists, when the notch length increases from 10 *mm* to 20 *mm*. From the results, the displacement amplitude increases when the notch angle increases from 15 degrees to 45 degrees, when the orientation is located at approximately 90 degrees. However, the amplitude decreases when the notch angle increases from 45 degrees to 75 degrees, despite increase in the axial direction (notch width). The results from the spacing of 20 degrees and 15 degrees between the two transducers are very close to each other for the different notch sizes. This indicates that reliable results for defect detection can be achieved using the transducer array with spacing within the range between 20 degrees and 15 degrees.

4. Experimental validation

In order to verify the related FE models, an experimental set-up was designed, as shown in Fig. 14. The torsional wave mode T(0,1) was excited by a tool composed

(a) N15 degrees×10 *mm*

(b) N45 degrees×10 *mm*

(c) N75 degrees×10 *mm*
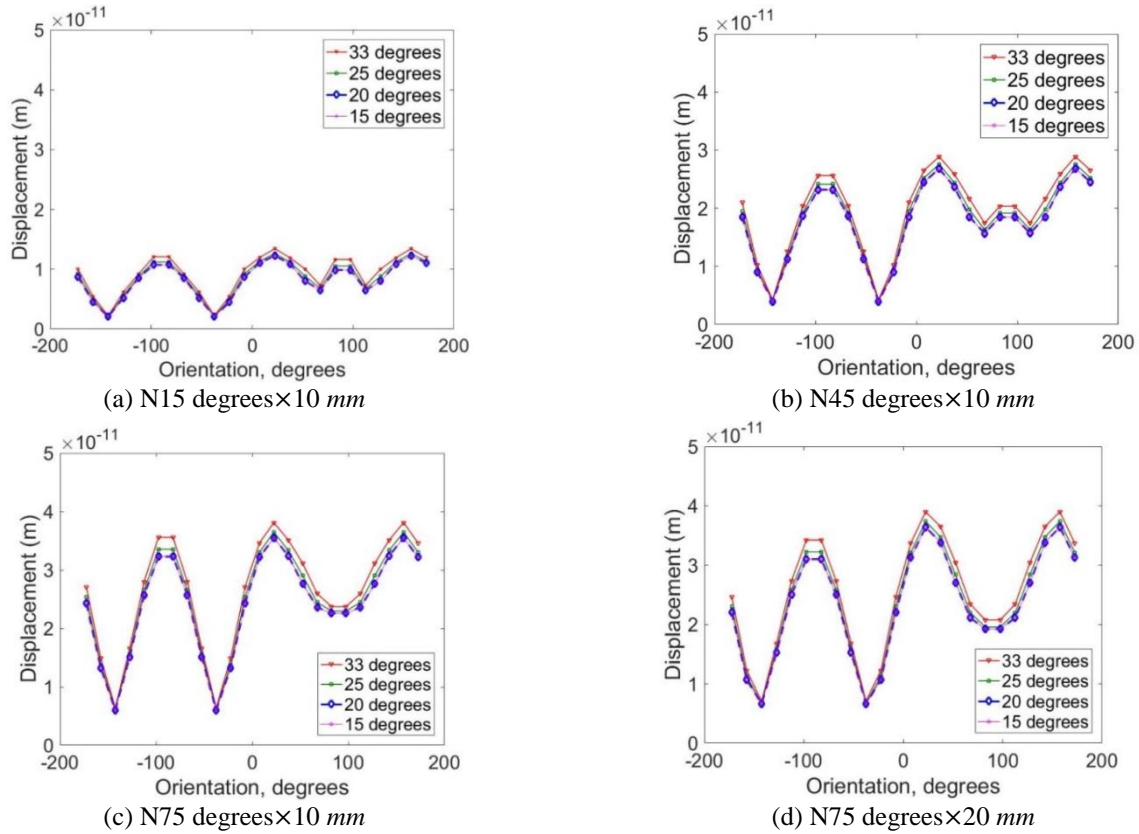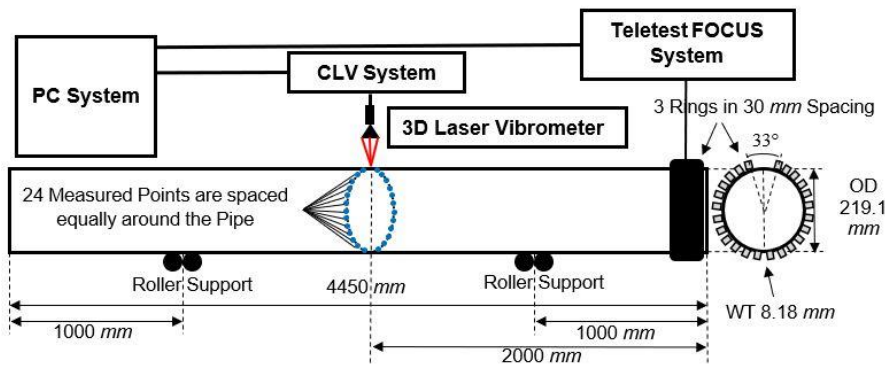
(d) N75 degrees×20 *mm*

Fig. 13 Reflection displacement amplitudes for various notches with different sizes using an array with a gap reducing from 33 degrees to 15 degrees

(a) Schematic diagram of experimental set-up

(b) Experimental transmitters with a gap of 33 degrees

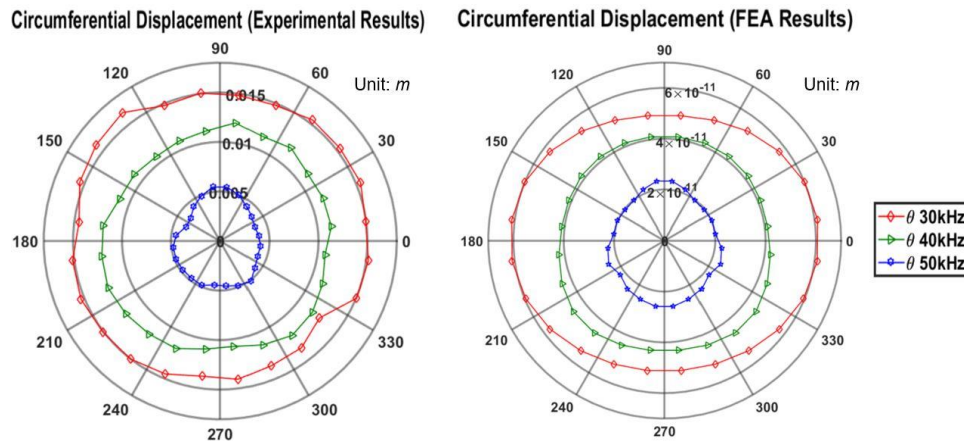Fig. 14 Experimental set-up for FE modelling validation

Fig. 15 Relative circumferential displacements from experimental studies and FE simulations

of three circumferential arrays with 24 transducers per ring array, where a gap of 33 degrees between start and end transducers in the array exists. A steel pipe of 4450 *mm* long, 8 inches (219.1 *mm*) in outer diameter (OD), and schedule 40 with wall thickness (WT) of 8.18 *mm* was used for testing. The array of transmitters was placed at the pipe end. The receiving array comprises a total of 24 points are equally spaced around the pipe and located at 2000 *mm* away from the pipe end. A CLV-3D laser vibrometer system was used to measure the amplitude of displacements in the circumferential direction at a wider range of frequencies from 30 *kHz* to 50 *kHz*.

Fig. 15 shows a comparison of relative circumferential displacements obtained from experimental results and FE simulations through polar plots. The maximum amplitudes of the transmitter signal at all 24 receiver locations are adopted. As different scales were outputted by the experimental studies and the FE modelling, only the relative amplitudes between the differences are considered. The results indicate that the amplitudes of the reflected signal reduce in both experimental and numerical cases, as frequency increases from 30 *kHz* to 40 *kHz* and then to 50 *kHz*. In the case with the frequency at 30 *kHz*, the amplitude of circumferential displacement from the finite element modelling does not agree well with the corresponding experimental results, particularly when the angle ranges from 60 degrees to 120 degrees. However, the simulated results have a good agreement with the experimental results in the case with the frequency at 40 *kHz* and 50 *kHz*, respectively. Furthermore, a range of frequency from 20 *kHz* to 60 *kHz* was tested using this transducer array in experiments (Niu *et al.* 2017c). From the experimental results, the centre frequency of 37 *kHz* for excitation is proved to be the best operating frequency for pipe inspection. Thus, when the centre frequency of excited signal is reduced to 30 *kHz*, the performance of the transducer array may decline, and noise level may increase. Without consideration of the internal performance of transducers, a good agreement is found between the experimental results and the FE simulations, and the FE modelling for the guided wave propagation in the pipe are then verified from the experimental results.

5. Conclusions

This paper investigates the behaviour of various types of transducer array for pipe inspection using guided waves. A series of parameters are evaluated including the number of transducers per array, variations in array spacing and variability of transducer excitation. In this study, a schedule 40 steel pipe of 4450 *mm* long and 219.1 *mm* in diameter is adopted for the FE simulations and the associated experimental studies. The excitation signal is chosen at the frequency of 30 *kHz* to propagate along a steel pipe, generating the torsional wave mode T(0,1) with a family of flexural wave modes F(*n*,2). In the numerical simulations, various cases are discussed for the outputs of guided waves, including arrays with 24 piezoelectric transducers, torsional wave mode T(0,1) excitation and different gaps between start and end of transducers. The sensitivity of transducer array is then analysed for the cases with various spacing reducing from 33 to 15 degrees between the top two transducers. Signal processing is utilised for separating wave modes to analyse the wave mode interaction of T(0,1) and F(*n*,2). The influence of the dimensions of a notch in the pipe is also investigated for various arrangements of the transducer array. The results from the numerical simulations are then compared with the experimental results.

From the numerical simulations and experimental studies, following conclusions are noted:

• As an axisymmetric pipe, a circumferential array of 24 piezoelectric transducers with equal spacing between all the transducers can generate a single torsional wave mode T(0,1) without undesired F(*n*,2) flexural modes. In this case, the displacement amplitude is constant across all 24 receivers in the circumferential direction.

• With a low-frequency of 30 *kHz* excitation, the flexural wave mode F(1,2) has very low contribution for the cases of non-axisymmetric arrays with an odd spacing in the range between 20 and 15 degrees.

• The torsional wave mode T(0,1) combining with the flexural wave modes F(*n*,2) as well as the single mode T(0,1) show high sensitivity to the notch size in the

circumferential direction, but low sensitivity to the notch size in the axial direction.

• In the FE simulation with a notch, the distribution of displacement amplitude reflected from the notch in polar plots shows a composition of the wave modes T(0,1) and F(1,2), depending on the notch sizes in the circumferential direction.

Acknowledgments

References

Alleyne, D.N. and Cawley, P. (1997), "Long range propagation of Lamb waves in chemical plant pipework", *Mater. Eval.*, **55**(4), 504-508.

Alleyne, D.N. and Cawley, P. (1992), "The interaction of lamb waves with defects", *IEEE T. Ultrason.Ferr.*, **39**(3), 381-397.

Alleyne, D.N. and Cawley, P. (1996), "The excitation of Lamb waves in pipes using dry-coupled piezoelectric transducers", *J. Nondestruct. Eval.*, **15**(1), 11-20.

Alleyne, D.N., Lowe, M.J.S. and Cawley, P. (1998), "The reflection of guided waves from circumferential notches in pipes", *J. Appl. Mech.*, **65**(3), 635-641.

Alleyne, D.N., Pavlakovic, B., Lowe, M.J.S. and Cawley, P. (2001), "Rapid, long range inspection of chemical plant pipework using guided waves", *Key Eng. Mater.*, **270-273**, 635-641.

Catton, P. and Kleiner, D. (2005), "Employing the focusing of guided waves for the in-situ non-destructive testing of pipes", *Proceedings of the Conferenza Nazionale sulle Prove non Distruttive Monitoraggio Diagnostica, 11th Congresso Nazionale dell'AIPnD*, Milan, Italy, October.

Cawley, P. (2007), "Practical guided wave inspection and applications to structural health monitoring", *Proceedings of the 5th Australasian Congress on Applied Mechanics (ACAM 2007)*, Brisbane, Australia, December.

Cawley, P., Alleyne, D.N. and Chan, C.W. (1994), "Inspection of pipes", London, Patent No. WO 96/12951.

Davies, J. and Cawley, P. (2009), "The application of synthetic focusing for imaging crack-like defects in pipelines using guided waves", *IEEE T. Ultrason. Ferr.*, **56**(4), 759-771.

Demma, A., Cawley, P., Lowe, M., Roosenbrand, A.G. and Pavlakovic, B. (2004), "The reflection of guided waves from notches in pipes: a guide for interpreting corrosion measurements", *NDT&E Int.*, **37**(3),167-180.

Duan, W. and Kirby, R. (2015), "A numerical model for the scattering of elastic waves from a non-axisymmetric defect in a pipe", *Finite Elem. Anal. Des.*, **100**, 28-40.

Duan, W., Kirby, R. and Mudge, P., (2016), "On the scattering of elastic waves from a non-axisymmetric defect in a coated pipe", *Ultrasonic*, **65**, 228-241.

Duan, W., Kirby, R., Mudge, P. and Gan, T.H. (2016), "A one dimensional numerical approach for computing the eigenmodes of elastic waves in buried pipelines", *J. Sound Vib.*, **384**, 177-193.

Duan, W., Kirby, R. and Mudge, P. (2017), "On the scattering of torsional waves from axisymmetric defects in buried pipelines", *J. Acoust. Soc. Am.*, **141**(5), 3250-3261.

Fateri, S., Lowe, P.S., Engineer, B. and Boulgouris, N.V. (2015), "Investigation of ultrasonic guided waves interacting with piezoelectric transducers", *IEEE Sens. J.*, **15**(8), 4319-4328.

Gazis, D.C. (1959), "Three dimensional investigation of the propagation of waves in hollow circular cylinders. i. analytical foundation", *J. Acoust. Soc. Am.*, **31**(5), 568-573.

Hong, X., Song, G., Ruan, J., Zhang, Z., Wu, S. and Liu, G. (2016), "Active monitoring of pipeline tapered thread connection based on time reversal using piezoceramic transducers", *Smart Struct. Syst.*, **18**(4), 643-662.

Hua, J., Mu, J. and Rose, J.L. (2011), "Guided wave propagation in single and double layer hollow cylinders embedded in infinite media", *J. Acoust. Soc. Am.*, **129**(2), 691-700.

Izadpanah, S., Rashed, G.R. and Sodagar, S. (2008), "Using ultrasonic guided waves in evaluation of pipes", *Proceedings of the 2nd International Conference on Technical Inspection and NDT* (*TINDT 2008*), Tehran, Iran, October.

Jenal, R., Staszewski, W.J., Klepka, A. and UHL, T. (2010), "Structural damage detection using laser vibrometers", *Proceedings of the 2nd International Symposium on NDT in Aerospace*, Hamburg, Germany, November.

Karayannis, C.G., Voutetaki, M.E., Chalioris, C.E., Providakis, C.P. and Angeli, G.M. (2015), "Detection of flexural damage stages for RC beams using piezoelectric sensors (PZT)", *Smart Struct. Syst.*, **15**(4), 997-1018.

Lee H. and Sohn H. (2012), "Damage detection for pipeline structures using optic-based active sensing", *Smart Struct. Syst.*, **9**(5), 461-472.

Leinov, E., Lowe, M.J.S. and Cawley, P. (2015), "Investigation of guided wave propagation and attenuation in pipe buried in sand", *J. Sound Vib.*, **347**, 96-114.

Liu, Z., He, C., Wu, B., Wang, X. and Yang, S. (2006), "Circumferential and longitudinal defect detection using T(0, 1) mode excited by thickness shear mode piezoelectric elements", *Ultrasonic*, **44**(supplement), e1135-e1138.

Liu, Z. and Kleiner, Y. (2013), "State of the art review of inspection technologies for condition assessment of water pipes", *Measurement*, **46**(1), 1-15.

Løvstad, A. and Cawley, P. (2011), "The reflection of the fundamental torsional guided wave from multiple circular holes in pipes", *NDT & E Int.*, **44**(7), 553-562.

Lowe, P.S., Fateri, S., Sanderson, R. and Boulgouris, N.V. (2014), "Finite element modelling of the interaction of ultrasonic guided waves with coupled piezoelectric transducers", *Insight - Non-Destructive Test. Condition Monit.*, **56**(9), 505-509.

Luo, W. and Rose, J. (2007), "Phased array focusing with guided waves in a viscoelastic coated hollow cylinder", *J. Acoust. Soc. Am.*, **121**(4), 1945-1955.

Luo, W., Rose, J.L. and Kwun, H. (2005), "Circumferential shear horizontal wave axial-crack sizing in pipes", *Res. Nondestruct. Eval.,* **15**(4), 149-171.

Meitzler, A.H. (1961), "Mode coupling occurring in the propagation of elastic pulses in wires", *J. Acoust. Soc. Am.*, **33**(4), 435-445.

Miao, H., Huan, Q., Wang, Q. and Li, F. (2017), "Excitation and reception of single torsional wave T(0,1) mode in pipes using face-shear d24 piezoelectric ring array", *Smart Mater. Struct.*, **26**(2), 025021.

Mohr, W. and Holler, P. (1976), "On inspection of thin-walled

tubes for transverse and longitudinal flaws by guided ultrasonic waves", *IEEE T. Sonics Ultrasonics*, **23**(5), 369 - 373.

Mudge, P. (2001), "Field application of the Teletest long-range ultrasonic testing technique", *Insight - Non-Destructive Test. Condition Monit.*, **43**(2), 74-77.

Muggleton, J.M., Brennan, M.J. and Pinnington, R.J. (2002), "Wavenumber prediction of waves in buried pipes for water leak detection", *J. Sound Vib.*, **249**(5), 939-954.

Muralidharan, A., Balasubramaniam, K. and Krishnamurthy, C.V. (2008), "A migration based reconstruction algorithm for the imaging of defects in a plate using a compact array", *Smart Struct. Syst.*, **4**(4), 449-464.

Niu, X., Chen, H.P. and Marques, H.R. (2017a), "Piezoelectric transducer array optimization through simulation techniques for guided wave testing of cylindrical structures", *Proceedings of the 8th ECCOMAS Thematic Conference on Smart Structures and Materials (SMART 2017)*, Madrid, Spain, June.

Niu, X., Marques, H.R. and Chen, H.P. (2017b), "Sensitivity analysis of guided wave characters for transducer array optimisation on pipeline inspections", *Proceedings of the 2017 World Congress on Advances in Structural Engineering and Mechanics (ASEM17)*, Seoul, Korea, August.

Niu, X., Marques, H.R. and Chen, H.P. (2017c), "Transducer array optimisation for guided wave testing of pipes using finite element numerical simulations and experimental studies", *Proceedings of the 8th International Conference on Structural Health Monitoring of Intelligent Infrastructure (SHMII8)*, Brisbane, Australia, December.

Pavlakovic, B., Lowe, M.J.S., Alleyne, D.N. and Cawley, P. (1997), "DISPERSE: a general purpose program for creating dispersion curves", *Review of Progress in Quantitative Nondestructive Evaluation*, Springer, New York, USA, **16**, 185-192.

Rose, J.L. (2014), *Ultrasonic Guided Waves in Solid Media.* Cambridge University Press, Cambridge, UK.

Sharan, P.K., S, S., Chaitanya, S.K. and Maddi, H.K. (2015), "Long range ultrasonic testing - case studies", NDT-2015, Trivandrum, India. http://www.nde2015.com/papers-1/paper-83.pdf

Silk, M.G. and Bainton, K.F. (1979), "The propagation in metal tubing of ultrasonic wave modes equivalent to lamb waves", *Ultrasonics,* **17**(1), 11-19.

Sung, C.C. and Tien, S.C. (2015), "The study on piezoelectric transducers: theoretical analysis and experimental verification", *Smart Struct. Syst.*, **15**(4), 1063-1083.

Volker, A. and Vos, H. (2012), "Experimental results of guided wave travel time tomography", *Proceedings of the AIP Conference 1430,1968*, Burlington, VT, USA, May.

Yu, B., Yang, S., Gan, C. and Lei, H. (2013), "A new procedure for exploring the dispersion characteristics of longitudinal guided waves in a multi-layered tube with a weak interface", *J. Nondestruct. Eval.*, **32**(3), 263-276.

Zhou, W., Li, H. and Yuan, F.G. (2016), "An anisotropic ultrasonic transducer for Lamb wave applications", *Smart Struct. Syst.*, **17**(6), 1055-1065.